

A new mechanism of nucleophilic vinylic substitution and unexpected products in the reaction of chlorotrifluoroethylene with $[\text{Re}(\text{CO})_5]\text{Na}$ and $[\text{CpFe}(\text{CO})_2]\text{K}$

P.K. Sazonov^{a,*}, G.A. Artamkina^a, K.A. Lyssenko^b, I.P. Beletskaya^{a,*}

^a Moscow State University, Chemistry Department, Leninskie Gory 1, GSP-2, Moscow 119992, Russian Federation

^b A.N. Nesmeyanov Institute of Organoelement Compounds (INEOS), Russian Academy of Sciences, Vavilov Street 28, Moscow 119991, Russian Federation

Received 27 July 2005; received in revised form 13 December 2005; accepted 23 December 2005

Available online 28 February 2006

Abstract

The mechanism of chloride substitution in $\text{CF}_2=\text{CFCl}$ with $[\text{Re}(\text{CO})_5]^-$ and $[\text{CpFe}(\text{CO})_2]^-$ anions is investigated experimentally and theoretically. The substitution reaction begins with the nucleophile addition to $\text{CF}_2=\text{CFCl}$ producing the carbenoid anion $[\text{MCF}_2\text{CFCl}]^-$ (**A**) ($\text{M} = \text{Re}(\text{CO})_5, \text{CpFe}(\text{CO})_2$). This is shown by trapping the intermediate **A** with electrophiles – proton donor (*t*-BuOH) to give MCF_2CFClH or with $\text{CF}_2=\text{CFRe}(\text{CO})_5$ to give acylmetallate **III**, and by the formation of the substitution products $\text{CF}_2=\text{CFM}$ from the anion **A**, generated by the deprotonation of MCF_2CFClH with *t*-BuOK. 1,2-Shift of metal carbonyl group concerted with the α -elimination of chloride anion is proposed as the transformation pathway of carbenoid **A** into $\text{CF}_2=\text{CFM}$. A competing process of carbene insertion into $\text{Fe}-\text{C}\equiv\text{O}$ bond is proposed to explain the formation of $\text{Cp}(\text{CO})\text{FeCF}=\text{CFC}(\text{O})\text{OBu-}t$ (**XI**). The feasibility of these two pathways is confirmed by DFT (B3LYP/SDD and 6-31G*) calculations of the carbenes $[\text{MCF}_2\text{CF}]$ and carbenoid anions $[\text{MCF}_2\text{CFCl}]^-$. Transition states (TS) for 1,2-shift (+3.2 kcal/mol) and for nucleophilic addition at $\text{C}\equiv\text{O}$ ligand (+5.4 kcal/mol) are located for $[(\text{CO})_5\text{ReCF}_2\text{CFCl}]^-$, but only one TS corresponding to carbene insertion into $\text{Fe}-\text{C}\equiv\text{O}$ bond (+2.1 kcal/mol) is located for $[(\text{CO})_2\text{CpFeCF}_2\text{CFCl}]^-$. The formation of other newly observed products, $\text{F}(\text{CO})\text{CHFRe}(\text{CO})_5$ (**V**) and $\text{Cp}(\text{CO})_2\text{FeC}\equiv\text{CFc}(\text{CO})_2$ (**VIII**) is also discussed.

© 2006 Elsevier B.V. All rights reserved.

Keywords: Transition metal carbonyl anions; SNV reactions; 1,2-Shift (migration); Carbenoids; Iron; Rhenium; DFT calculations

1. Introduction

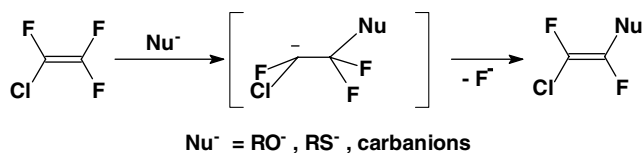
Probably no other class of organic reactions is as rich in mechanistic alternatives and mechanistic criteria to differentiate between them as nucleophilic vinylic substitution. At present more than 10 main types of reaction mechanisms are recognised [1], and other pathways are likely to be discovered in the future. However, most mechanistic studies of vinylic substitution [2] do not go beyond the basic set of “traditional” nucleophiles, – alkoxides, amines, thiolates and, to a minor extent, carbanions. The focus of our interest in vinylic

substitution is the influence of the particular nature of transition metal centered nucleophiles on the reaction mechanism. Such features of metal carbonyl anions as high reducing power and halogen affinity, the weakness of carbon-metal bond forming in the reaction, and the feasibility of reactions affecting the ligands ($\text{C}\equiv\text{O}$), let alone their practical importance as catalysts and reagents, make them an excellent model for our studies.

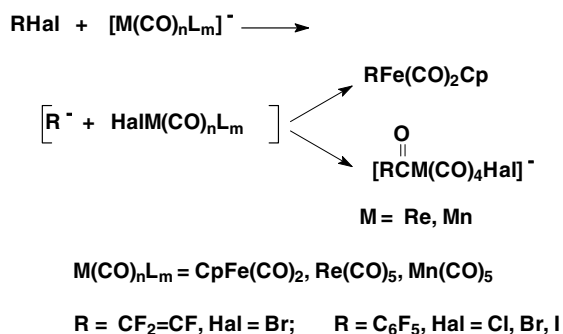
One of the basic mechanistic criteria in nucleophilic substitution at sp^2 -carbon atom is the element effect, the relative mobility of halogen leaving groups. Higher mobility of fluorine relative to other halogens is normal for the reactions with “traditional” nucleophiles, which follow the addition- β -elimination mechanism with the rate limiting addition step (Scheme 1) [1,2]. Yet, an “abnormal” leaving

* Corresponding authors. Tel./fax: +7 095 9393618.

E-mail addresses: beletska@org.chem.msu.ru, petr@elorg.chem.msu.ru (I.P. Beletskaya).



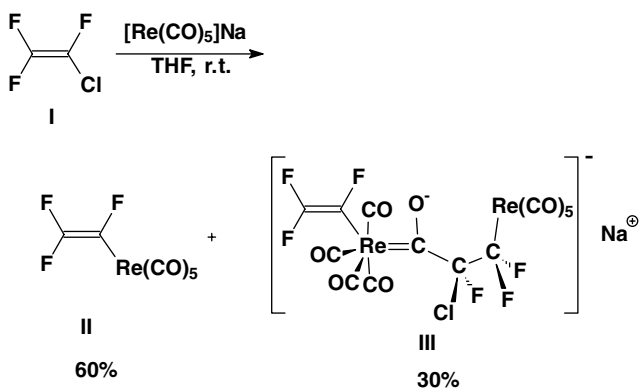
Scheme 1.



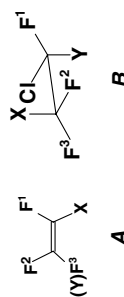
Scheme 2.

group effect ($\text{Hal} > \text{F}$, where $\text{Hal} = \text{Cl, Br, I}$) is frequently observed for metal-centered anions, cobaloximes and carbonylmetallates, in their reactions with vinylic and aromatic halides. As we have previously shown [3,4], such reactivity pattern of polyfluorinated aryl and vinyl halides is in fact a manifestation of a different reaction mechanism – halogen–metal exchange (HME) (Scheme 2). The intermediate carbanion interaction with metal carbonyl halide gives the nucleophilic substitution (NS) products. In case of rhenium and manganese carbonyl halides the carbanion adds to the carbonyl ligand forming halo(acyl)metallate anions instead of σ -alkenyl complexes.

The present work, however, shows that vinylic substitution has still a few surprises to offer, and even in such a simple system as $\text{CF}_2=\text{CFHal}$ there is an alternative pathway for the substitution of the heavy halogen. It is known that the reaction of chlorotrifluoroethylene with $[\text{CpFe}(\text{CO})_2]\text{K}$ and $[\text{Re}(\text{CO})_5]\text{Na}$ leads only to the substitution of chloride anion [5]. One might suppose that it also follows the halophilic pathway, but an entirely different mechanism operates in this reaction. Our results point to the carbenoid $[\text{L}(\text{CO})_n\text{MCF}_2\text{CFCl}]^-$ (A) as the key intermediate, which



Scheme 3.

Table 1
NMR (^{19}F and ^1H) spectral data, THF, 23 °C

Compound	Sub-system	X	Y	$\delta_{\text{F}}/\text{ppm} (J_{\text{H-F}}/\text{Hz})$		$\delta_{\text{H}}/\text{ppm} (J_{\text{H-F}}/\text{Hz})$				
				F ¹	F ²	F ³	$^n J_{\text{F-F}}/\text{Hz}$	$^m J_{\text{F-F}}/\text{Hz}$	$^p J_{\text{F-F}}/\text{Hz}$	
II	A	Re(CO) ₅	–	–144.52 dd	–91.05 dd	–124.03 dd	113	92	32	–
III-18-crown-6 ^a	A	See Scheme 3	–	–147.12 dd	–97.03 dd	–126.67 dd	111	98	30	–
	B		–	–58.69 dd, br	–64.46 d, br	<10	≈288	≈12	–	–
IV	B	Re(CO) ₅	H	–136.46 dt ($J_{\text{H-F}}$ 51)	–55.0 ddd ($J_{\text{H-F}}$ 10)	–67.48 ddd ($J_{\text{H-F}}$ 8)	16	299	14	5.974 ddd ($J_{\text{H-F}}$ 52, 10, 8)
VI	B	<i>t</i> -Bu(CO)Re(CO) ₄	H	–136.81 dt ($J_{\text{H-F}}$ 48)	–76.5 d br	–84.9 d, br	≈17	≈280	≈17	–
IX	B	Cp(CO) ₂ Fe	H	–135.23 ddd ($J_{\text{H-F}}$ 48)	–49.74 dd	–56.91 dt ($J_{\text{H-F}}$ 17)	17	236	22	6.215 dd ($J_{\text{H-F}}$ 48, 17); 5.127 s (Cp)
X	B	<i>t</i> -BuO	H	–152.23 dt ($J_{\text{H-F}}$ 48)	–78.2 dd	–79.19 ddd ($J_{\text{H-F}}$ 5)	12	142	12	6.35 d br ($J_{\text{H-F}}$ 48); 1.449 s (<i>t</i> -Bu)
XI	A	See Fig. 1	–	–44.70 d	–140.27 d	–	–	–	15	4.652 s (Cp); 1.343 s (<i>t</i> -Bu)

^a –64 °C.

is transformed to the substitution products via 1,2-shift of the metal carbonyl group. The proposed mechanism is validated by computational modeling of the corresponding intermediates and transition states.

Reactions were usually carried out directly in a NMR sample tube, so that the product composition, including the unstable and volatile compounds, could be determined directly from NMR spectra. Trapping of the intermediate carbanionic species with proton donors, that has often helped us to understand the reaction mechanism [3,4], is another technique used in the current study. We have also examined the action of *t*-BuOK(Na)/*t*-BuOH on the saturated adducts **IV** and **IX** in order to trace the genetic relationship between the reaction products.

2. Results and discussion

2.1. Reaction of $CF_2=CFCl$ (**I**) with $[Re(CO)_5]Na$

The ^{19}F NMR spectrum of the reaction solution showed that besides the $CF_2=CFRe(CO)_5$ product (**II**, 60%), previously isolated from this reaction [5], another product is also formed (Scheme 3). In the ^{19}F NMR spectrum of this new compound (Table 1) one can see both resonances belonging to trifluorovinyl group and those belonging to $XCF_2-CFClY$ fragment, and in IR (Table 2) and ^{13}C NMR spectra patterns characteristic for neutral $XRe(CO)_5$ and anionic *cis*- $X_2Re(CO)_4$ complexes¹ [3,4,6,7]. The above data allowed to identify it as a rhenium acylmetallate salt (**III**, 30%). Complex of **III** with 18-crown-6 and dioxane was precipitated from the reaction mixture as a yellow crystalline solid.

Complex **III** is an obvious indication of a carbanionic σ -adduct intermediate $[(CO)_5ReCF_2CFCl]^-$ (**A**) taking part in the reaction. It may result only from nucleophilic addition of intermediate **A** to CO ligand of complex **II** (Scheme 4). Nucleophilic addition to CO ligand is highly characteristic for metal carbonyls, especially electrophilic complexes such as $RRe(CO)_5$ ($R = Hal, R_f$ or other EWG-group) [6,7].

The role of anionic σ -adduct **A** as an intermediate in the reaction was further confirmed when the reaction was carried out in the presence of *t*-BuOH (2 eq), a proton donor, which can effectively trap carbanions [3,4]. In that “anion trapping” experiment (Scheme 5) the nucleophilic substitution products **II** and **III** were not observed in the reaction mixture, instead the saturated adduct (**IV**, 35%) was formed, confirming the addition of $[Re(CO)_5]^-$ anion to **I** at the CF_2 -site. The formation of other products, α -metallated fluoroanhydride $F(CO)CHRe(CO)_5$ (**V**, 35%), isobutene² (40%)

¹ Two axial $C\equiv O$ groups in *cis*- $X_2Re(CO)_4$ fragment are diastereotopic because of the presence of a chiral centre in the structure of **III** ($CFCl$ group), and hence $X_2Re(CO)_4$ gives four signals of equal intensity in ^{13}C NMR spectrum instead of 1:2:1 pattern typical of such complexes in symmetrical ligand environment.

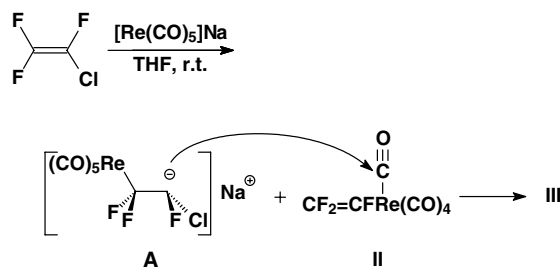
² Isobutene was identified by its characteristic signals in 1H NMR (δ_H , ppm: 1.676, 4.609, J_{H-H} 1.2 Hz) and ^{13}C NMR spectra (δ_C , ppm: 24.12, 110.96, 142.55).

Table 2
IR spectra of metal carbonyl complexes

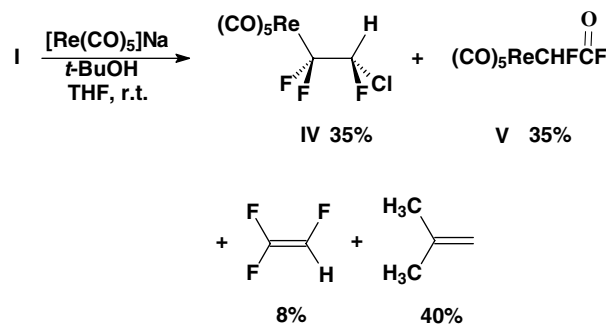
Compound	IR-spectrum, ^a ν/cm^{-1}		
	$\nu_{C=O}$	$\nu_{C=C}$	$\nu_{C\equiv O}$
II	–	1713 m	2011 vs, 2038 vs, 2083 m, 2152 m
III^b	1610 m br	1702 m	1927 vs, 1970 sh, 1984 vs, 2035 vs, 2087 s, 2149 m
IV	–	–	2020 sh, 2037 vs, 2082 m, 2152 m
V	1833 s	–	2013 vs, 2037 vs, 2082 m, 2151 m
VII	–	1717 m	1994 vs, 2044 vs
VIII	–	–	1984 vs, 2027 vs, 2043 vs
IX	–	–	1993 vs, 2044 vs
XI	1605 s	–	1967 vs
XII	1655 s, br	–	1987 vs, 2039 vs

^a THF, r.t., $l_{cell} = 0.02$ cm, range 1600–2300 cm^{-1} .

^b In the presence of 18-crown-6.



Scheme 4.

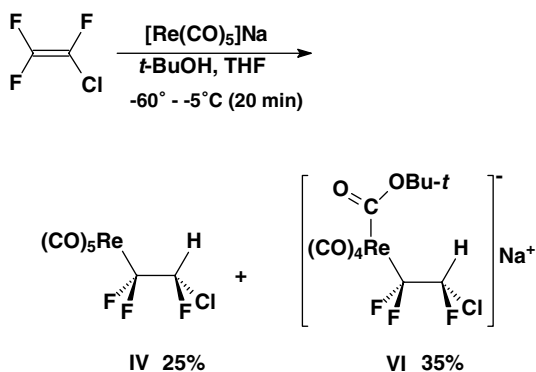


Scheme 5.

and $CF_2=CFH$ is not so easy to explain, and will be discussed later in Section 2.2.

The same reaction when monitored by ^{19}F NMR at low temperature (-60 to -5 °C) gave only two products. One was the already mentioned **IV**, for the other product structure **VI** might be surmised³ (Scheme 6). On heating the reaction mixture to r.t. (30 min) the signals ascribed to **VI** disappeared, and signals belonging to **V** and $CF_2=CFH$ became visible in ^{19}F NMR spectrum.

³ It exhibited a signal pattern similar to **IV**, but with slightly different chemical shifts (Table 1). Taking into account the tendency of $RRe(CO)_5$ complexes to add nucleophiles at the *cis*-carbonyl ligand it might be well to surmise the structure **VI** for this intermediate.



Scheme 6.

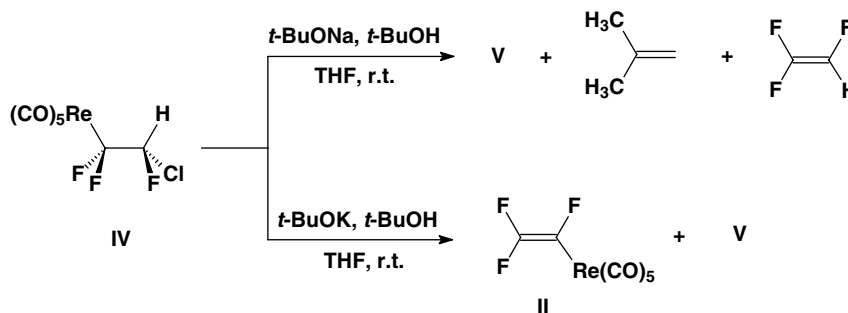
It is reasonable to suppose that the anionic σ -adduct **A** can be generated by the deprotonation of the saturated adduct **IV**, and thus the chemistry associated with this intermediate can be reproduced. Therefore, we studied the reaction of **IV** with *t*-BuONa(K)/*t*-BuOH mixture (Scheme 7). The result depended on the counterion. The reaction of **IV** with *t*-BuOK produced σ -vinylic complex **II** together with **V** in 2:1 ratio. In case of *t*-BuONa the products {**V**, isobutylene, a minor amount of $\text{CF}_2=\text{CFH}$ and no σ -vinylic complex **II** (Scheme 7)}, reproduce the

composition observed in the reaction of $[\text{Re}(\text{CO})_5]\text{Na}$ with **I** in the presence of *t*-BuOH (Scheme 5).

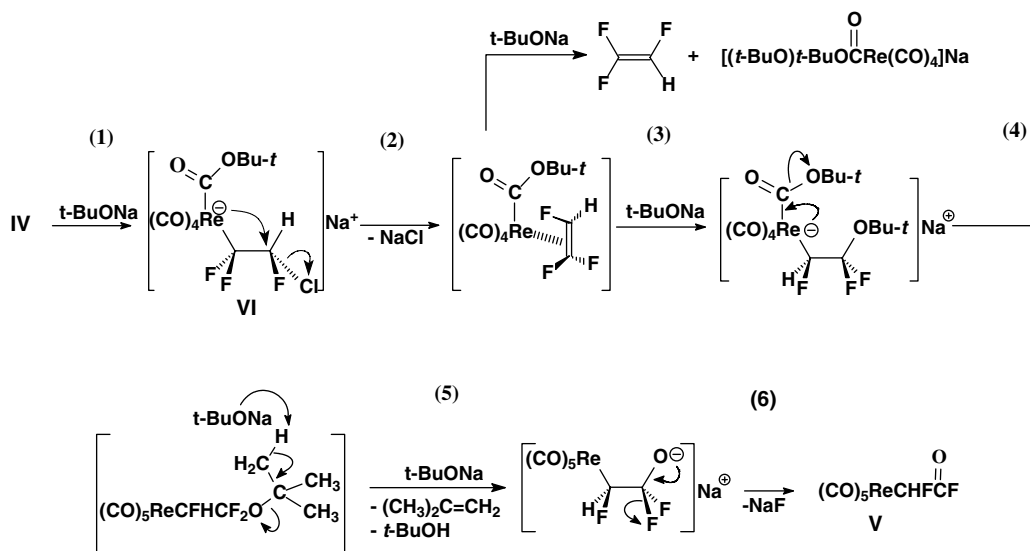
2.2. Possible mechanism for the formation of $(\text{CO})_5\text{ReCHF}(\text{CO})\text{F}$ (**V**), isobutylene and $\text{CF}_2=\text{CFH}$

As demonstrated by the low temperature experiment (Scheme 6) and the reaction of **IV** with *t*-BuONa (Scheme 7), fluoroanhydride **V**, isobutylene and $\text{CF}_2=\text{CFH}$ are formed together from the saturated adduct **IV** via the intermediate **VI**, i.e., in the process beginning with the addition of *t*-BuONa to the CO-ligand of **IV**. The sequence of transformations following may be rationalized as shown in Scheme 8.

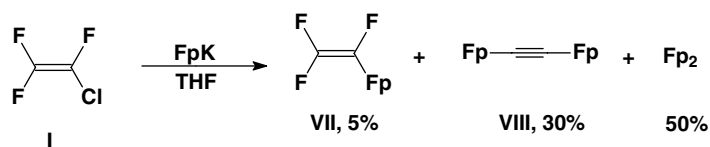
Stage (2) of this mechanism involves γ -elimination of chloride anion from the acylmetallate **VI**, a reaction reverse to the nucleophilic attack on a π -coordinated alkene. The nucleophilic attack of *t*-BuONa on the π -complex of $\text{CF}_2=\text{CFH}$ may result either in the substitution of this weakly bound ligand, producing free $\text{CF}_2=\text{CFH}$, or it may result in the nucleophilic addition of *t*-BuO⁻ to the coordinated fluoroalkene (**3**). The sequence is completed by base induced elimination of isobutylene from *tert*-butyl-fluoroalkyl ether (**5**), leading to the fluoroanhydride



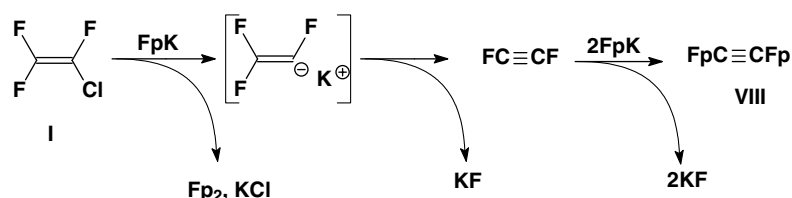
Scheme 7.



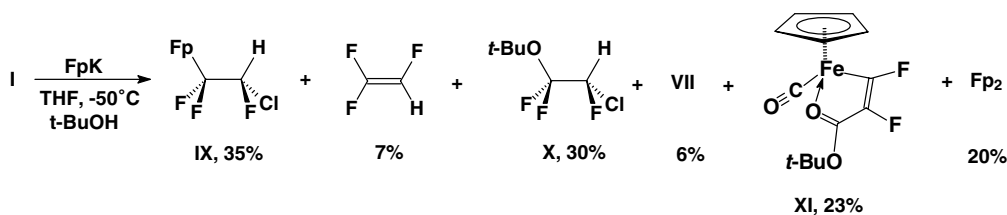
Scheme 8.



Scheme 9.



Scheme 10.



Scheme 11.

V (6), a transformation well known in fluorine chemistry [8].

2.3. Reaction of $\text{CF}_2=\text{CFCl}$ (I) with $[\text{CpFe}(\text{CO})_2]\text{K}$ (FpK)

Just as described by Bruce et al. [5] the reaction of FpK with I gives no more than 5% of the corresponding NS product VII (Scheme 9). No other fluorine-containing compounds were observed by ^{19}F NMR, however there was a non-fluorinated product not reported previously – a di-metal substituted acetylene VIII (30%). The IR-spectrum of acetylene VIII in metal carbonyl region consists not of two, which is typical for other FpX complexes, but of three bands of unequal intensity (Table 2). A similar spectral pattern has been observed for the ruthenium analogue of complex VIII, and it was suggested that *sin* and *anti* rotamers of the complex give separate bands in IR-spectrum [9].

Formation of acetylene VIII is a characteristic signature of the corresponding fluoroalkenyl carbanion, the $[\text{CF}_2=\text{CF}]^-$ anion, which can eliminate β -fluoride to give the “superelectrophilic” difluoroacetylene (Scheme 10).

The situation changed significantly when the reaction was carried out in the presence of *t*-BuOH (Scheme 11):

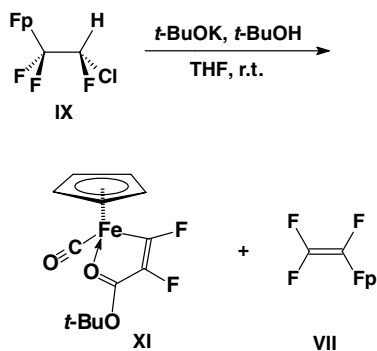
- (a) The formation of acetylene VIII was suppressed completely, which, together with the observation of $\text{CF}_2=\text{CFH}$ (7%), was only to be expected for a process involving $[\text{CF}_2=\text{CF}]^-$ carbanion (Scheme 10).

- (b) The observation of saturated adduct⁴ (IX, 35%) indicates that $[\text{FpCF}_2\text{CFCl}]^-$ intermediate (A-Fe) is formed in the course of the reaction, i.e., it confirms the FpK addition to the CF_2 -group of I.
- (c) The formation of the NS product VII (6%) seems to be unaffected by proton donor.
- (d) A new metallocycle product XI (23%) is formed. Formation of metallocycle XI largely depends upon the nature of the cation in the carbonylate salt. The same reaction carried out with FpLi instead of FpK afforded products IX (45%), VII (5%), $\text{CF}_2=\text{CFH}$ (5%) and Fp_2 dimer (40%), but gave no complex XI.

The treatment of the saturated adduct IX with *t*-BuOK also produces metallocycle XI together with σ -vinyl complex VII (Scheme 12).

The structure of XI was confirmed by single-crystal X-ray diffraction analysis and is shown in Fig. 1. Complex XI has a slightly distorted piano-stool geometry. Its chief peculiarity is the coordination of acyl oxygen to iron, forming a five-membered conjugated cycle. The metallocycle is characterized by flattened envelope conformation with the deviation of the O(1) atom by 0.064(3) Å from the plane of the remaining atoms. Several examples of similar metallocyclic iron complexes have already been described

⁴ The saturated adduct IX appears to be extremely moisture sensitive unlike other organofluorine metal carbonyl derivatives. The crystals of IX become blurred in the open air in a matter of minutes, resulting in a brownish oil mainly consisting of $\text{Fp}(\text{CO})\text{CHFCI}$ (XII).



Scheme 12.

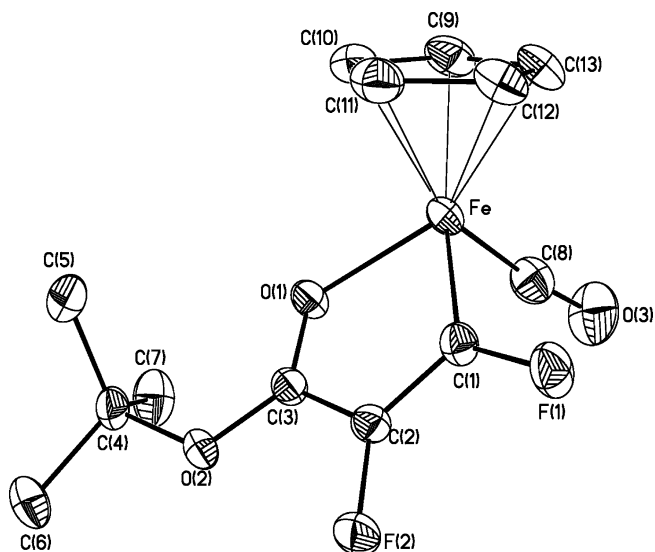


Fig. 1. A general view of the molecular structure of metallocycle XI (50% probability ellipsoids). Selected bond distances (Å): Fe–C(1) 1.903(2), Fe–O(1) 2.012(2), Fe–C(8) 1.755(2), O(1)–C(3) 1.257(3), C(1)–C(2) 1.347(3), C(2)–C(3) 1.432(3), O(2)–C(3) 1.312(3); and bond angles (°): C(8)–Fe–C(1) 91.8(1), C(8)–Fe–O(1) 99.92(9), C(1)–Fe–O(1) 81.14(8).

[10]. A mechanism proposed in the literature for their formation usually consists in (a) attack of the nucleophile at the CO ligand of σ -aryl complex (σ -vinyl in our case); (b) γ -elimination of leaving group resulting in a π -coordinated aryne (in our case it would be alkyne); (c) intramolec-

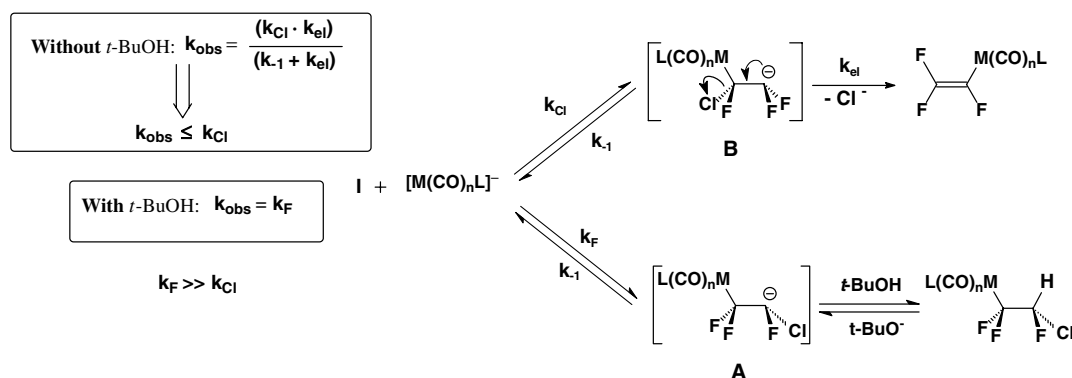
ular insertion of a coordinated aryne (alkyne) into Fe–C bond of R(CO)Fe group [10]. However, this mechanism is inconsistent with our observation, that the action of *t*-BuOK on iron σ -vinyl complex VII did not give any traceable products. The mechanism that would be acceptable has to take into account the transformation of the saturated adduct IX into complex XI under the action of *t*-BuOK (Scheme 12), and this suggests [FpCF₂CFCl][−] anion (A–Fe) as an intermediate.

2.4. The mechanism of chloride substitution in CF₂=CFCl (I) by metal carbonyl anions

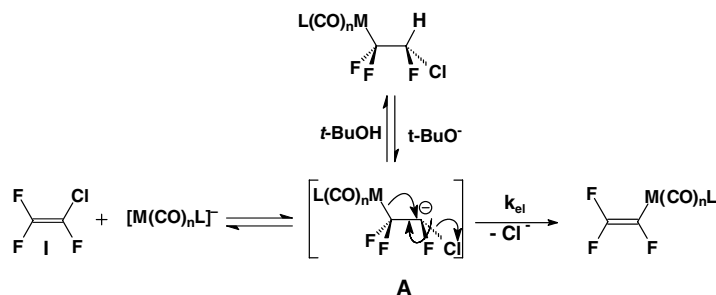
We can exclude the HME pathway (Scheme 2) from the start, as it would have produced haloacylrhenate [CF₂=CF(CO)Re(CO)₄Cl]Na instead of σ -vinyl complex II actually formed in the reaction with [Re(CO)₅]Na. The results of anion trapping experiments both for iron (Scheme 11) and rhenium (Schemes 5 and 6) are not consistent with the HME mechanism either. On the other hand: (a) formation of complex III (Scheme 3); (b) formation of saturated adducts IV (Scheme 5) and IX (Scheme 11) in the presence of *t*-BuOH, while the formation of NS products II and III is completely suppressed; (c) formation of NS products II and VII directly from the corresponding adducts IV and IX under the action of *t*-BuOK (Schemes 7 and 12) – all this points to carbanionic σ -adduct [MCF₂CFCl][−] (A) as the intermediate on the NS pathway.

The problem, however, is that anion A cannot transform into NS products II and VII by β -elimination of a leaving group, which would be β -elimination of fluoride as is the case with “ordinary” nucleophiles (RO[−], RS[−], R₂N[−], carbanions, Scheme 1). There must be some other pathway for the transformation of the intermediate A, much more facile than β -elimination of fluoride.

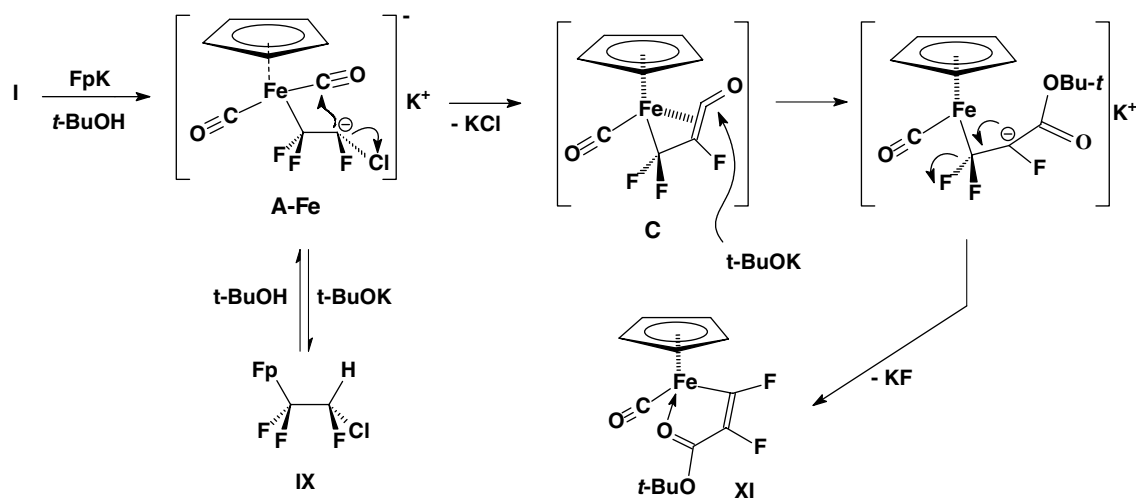
A question arises: could the exclusive substitution of chloride in I be explained by a mechanism with parallel and reversible formation of two isomeric carbanions A and B (Scheme 13)? The NS products can be formed from a less stable carbanion B, while the anion trap protonates the more stable carbanion A present in much higher concentration.



Scheme 13.



Scheme 14.



Scheme 15.

Our answer is no. Firstly, if this scheme is true, it is difficult to conceive how NS products could be formed directly from the saturated adducts **IV** and **IX** under the action of *t*-BuOK. Secondly, we have shown that the rate of the reaction of **I** with $[\text{Re}(\text{CO})_5]\text{Na}$ does not change in the presence of *t*-BuOH ($k_2 = 0.7 \pm 0.15 \text{ l mol}^{-1} \text{ s}^{-1}$), while a significant rate increase (proportional to $k_{\text{F}}/k_{\text{Cl}}$) has to be expected according to Scheme 13. And finally, this mechanism does not explain the formation of metallocycle product **XI** from carbanion **A**.

Carbanion intermediate **A**, like all α -halogen-substituted carbanions [11], is a carbenoid, and this is the key point in understanding the reaction mechanism. Its transformation into the NS products **II** or **VII** can proceed via 1,2-shift of metal carbonyl group concerted with α -elimination of chloride anion (Scheme 14).

While 1,2-shift in carbanions is considered not feasible due to the antiaromaticity of the corresponding 4-electron transition state, no molecular orbital symmetry restrictions apply to the 1,2-shift in a carbenoid if it is concerted with the elimination of chloride anion [12]. It is the key step in Fritsch–Buttenberg–Wiechell rearrangement, and is analogous to Beckmann rearrangement of oximes [12]. In case of free carbenes the 1,2-shift of the β -substituent to the carbene centre is usually a rapid process [13]. The ease of this rearrangement increases for β -substituents forming weak

bonds to carbon, such as silicon [14,15]. The same must be true for transition metal groups, $\text{Re}(\text{CO})_5$ and $\text{Fe}(\text{CO})_2\text{Cp}$. Concerted 1,2-shift of metal carbonyl group appears to provide additional driving force for the α -elimination of chloride anion, since the analogous carbanion intermediates in the reactions of **I** with sulphur or oxygen nucleophiles do not eliminate chloride (Scheme 1).

Moreover, if we consider that carbenes (and consequently carbenoids) are easily inserted into metal–C \equiv O bond [16], formation of metallocycle **XI** from the carbenoid anion **A-Fe** can be also explained. Insertion of the carbene equivalent into Fe–C \equiv O bond will produce the iron ketene complex **C** (Scheme 15). Nucleophilic addition of alkoxide

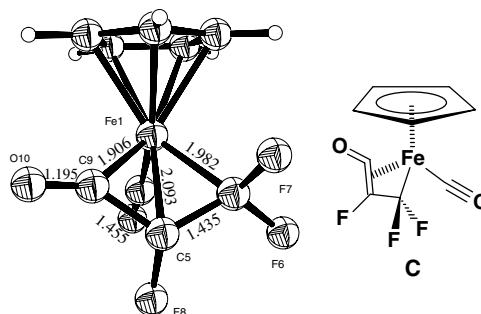


Fig. 2. The calculated structure of ketene intermediate **C** (bond lengths in Å).

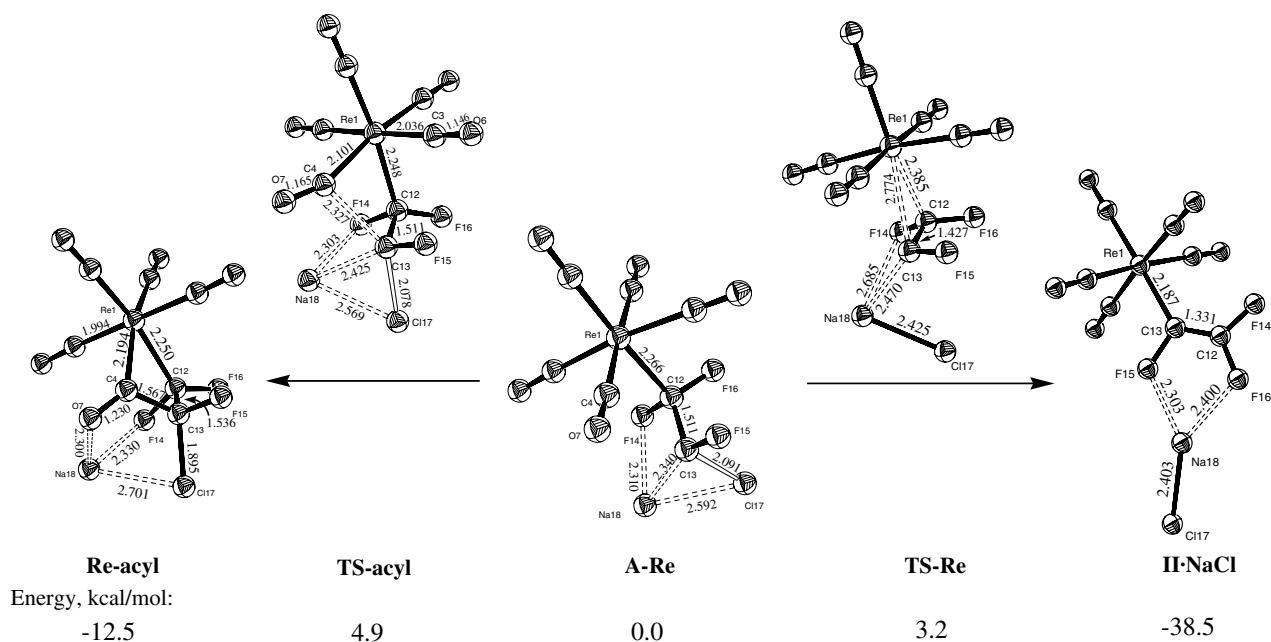


Fig. 3. The calculated structures and energies of rhenium carbenoid $[(\text{CO})_5\text{ReCF}_2\text{CFCl}]\text{Na}$ (**A-Re**), its transformation products (**II·NaCl** and **Re-acyl**) and the corresponding transition states (**TS-Re** and **TS-acyl**).

to iron ketene complexes has been described [17]. It is directed at the central carbon atom of ketene ligand and gives alkoxy carbonyl iron complexes. Thus, the reaction of **C** with *t*-BuOK will give the metallacycle **XI**, and the formation of **XI** supports the proposed carbenoid mechanism (Scheme 14).

2.5. DFT study of carbenes $[\text{MCF}_2\text{CF}]$ and carbenoids $[\text{MCF}_2\text{CFCl}]\text{Na}$ ($M = \text{Re}(\text{CO})_5\text{Na}$ and $\text{CpFe}(\text{CO})_2$): 1,2-shift via carbene insertion into metal–CO bond

Carbenes and more recently carbenoids [11] have been the subject of extensive quantum chemical studies, yet very little data are available on 1,2-shift of groups other than hydrogen or simple organic radicals. As for the β -element substituted carbenes we can find some data only for silicon. It was shown (at MP2 or B3LYP levels of theory) that β -silicon substituted carbenes represent no minima on potential energy surface rearranging to the corresponding alkenes without an activation barrier [14,15].

The calculation method used in this study (B3LYP/SDD(Fe, Re) 6-31G(d) for all other elements) has shown very good performance in various organometallic systems [18]. We have checked its adequacy for the systems under consideration by computing the structures of iron metallacycle **XI** and halo(acyl)rhenate anion $[\text{CF}_2=\text{CF}(\text{CO})\text{Re}(\text{CO})_4\text{Br}]^-$ [4]. In both cases the computed structures were in good agreement with the X-ray data.

At first we chose the carbenes $(\text{CO})_5\text{ReCF}_2\text{CF}$: and FpCF_2CF : as more simple models of the key intermediate in the proposed mechanism – carbenoid **A**. However, for the free carbenes no energy minima could be located. Both

carbenes rearrange in the process of geometry optimisation, but rearrangement pathways are different for iron and rhenium. 1,2-Migration of $\text{Re}(\text{CO})_5$ group in $(\text{CO})_5\text{ReCF}_2\text{CF}$: results in σ -vinyl complex (**II**) ($\Delta E = 46.1$ kcal/mol),⁵ but in its iron analogue carbene inserts into Fe–CO bond ($\Delta E = 22.5$ kcal/mol). The resulting structure (Fig. 2), may be regarded as iron ketene complex, which was proposed as an intermediate (**C**) in the formation of metallacycle **XI** (Scheme 15).

The calculation of rhenium analogue of ketene complex **C** showed that its formation from $(\text{CO})_5\text{ReCF}_2\text{CF}$: is less exothermic than **C** from FpCF_2CF : by 5.4 kcal/mol. This, however, does not seem to be the only reason for the preferred insertion in FpCF_2CF :. Because of the shorter Fe–C bonds and greater steric crowding imposed by Cp ring, the 1,2-migration path intersects with the slopes of the “hollow” corresponding to ketene complex **C**.

In contrast to free carbenes energy minima correspond to the carbenoids $[(\text{CO})_5\text{ReCF}_2\text{CFCl}]\text{Na}$ (**A-Re**) and $[\text{FpCF}_2\text{CFCl}]\text{Na}$ (**A-Fe**). A number of isomeric structures for these carbenoids were located, differing in the OC–Fe–CF₂–CFCl dihedral angle and the coordination mode of Na (with CF or CO bonds). The most stable are shown in Figs. 3 and 4. The structures show that they are typical carbenoids, with elongated C–Cl bond (2.18 Å and 2.09 Å for **A-Fe** and **A-Re**, respectively) and a three-centre coordination of Na cation with Cl, carbenoid-C and β -F atoms.

⁵ Relative to the energy of the starting carbene optimised with $\text{Re}(\text{Fe})\text{CF}_2\text{CF}$: angle constrained to 110° (obtained in molecular mechanics geometry optimisation with mm+ force field).

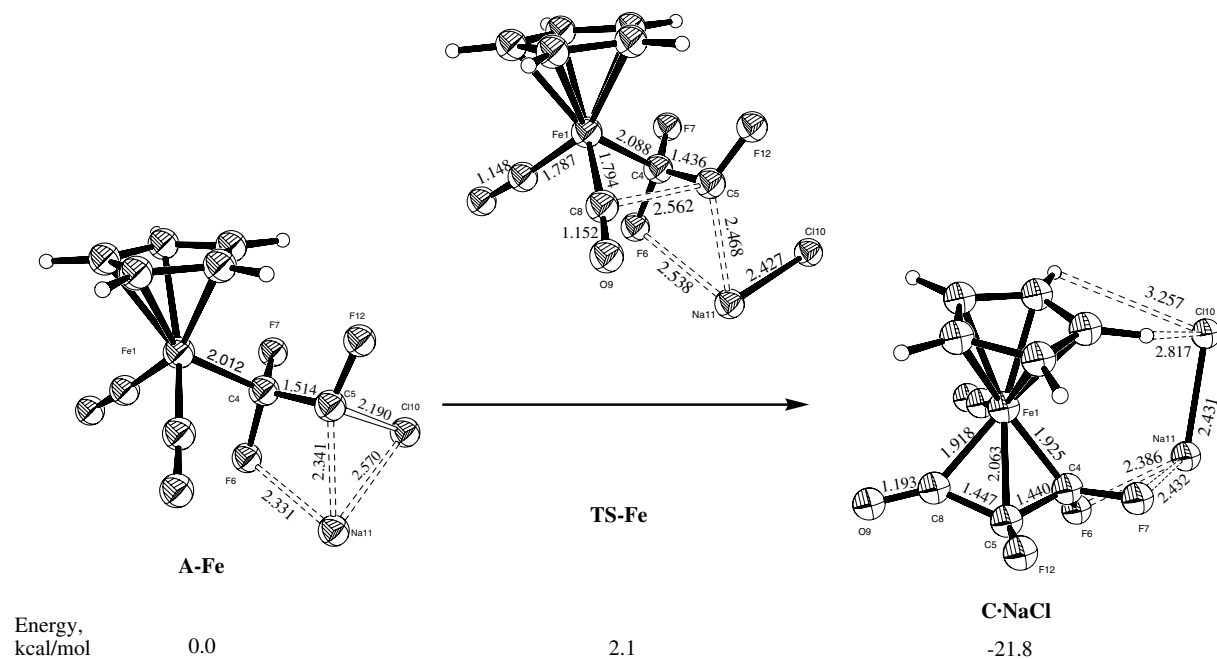


Fig. 4. The calculated structures and energies of iron carbenoid [(CO)₂CpFeCF₂CFCl]Na (**A-Fe**), ketene complex (**C·NaCl**) and the connecting transition state (**TS-Fe**).

A transition state (TS) for 1,2-migration of Re(CO)₅ group (**TS-Re** in Fig. 3) was easily located. The activation barrier for 1,2-migration is only 3.2 kcal/mol, and **TS-Re** can be characterized as early and asymmetrical. The developing Re–CF bond is much longer (2.77 Å), than the breaking Re–CF₂ bond (2.38 Å). Another TS (**TS-acyl** in Fig. 3) higher in energy (4.9 kcal/mol) than **TS-Re** corresponds to the attack of carbenoid anion at the CO ligand, however, it is not an insertion of carbene as it does not lead to the rhenium ketene complex analogous to **C**. It corresponds instead to the *intramolecular* nucleophilic addition of the carbanion to CO group, resulting in the acylrhenate salt (**Re-acyl** in Fig. 3). We see here obvious parallel with the *intermolecular* nucleophilic addition of [(CO)₅ReCF₂CFCl]Na to the CO ligand of **II** observed in the experiment (Scheme 4).

Only one TS (**TS-Fe** in Fig. 4) was found for iron carbenoid **A-Fe** corresponding to the insertion of carbene into the Fe–CO bond and leading to the cyclic ketene product **C**, or rather its complex with NaCl (**C·NaCl** in Fig. 4). It is an extremely low lying (2.1 kcal/mol above **A-Fe**) and early TS, with a very little change in Fe–C≡O angle and bond lengths. The distance between CO group and the carbenoid carbon in **TS-Fe** is as long as 2.56 Å.

The most important conclusion that follows from the above data are that different transformation pathways are predicted for rhenium and iron carbenoids. It qualitatively reproduces the different chemistries characteristic of [Re(CO)₅]Na and [CpFe(CO)₂]K in the reaction with **I**. Thus, the computational results support the proposed mechanisms (Schemes 14 and 15) with the carbenoid anions as the key intermediates.

3. Conclusions

The title reaction became a classical example of the so-called “abnormal halogen leaving group effect” – the preferred substitution of a heavy halogen in a vinyl halide usually associated with the metal-centered nucleophiles [19]. The present study shows that this reaction is a clear case of the “carbenoid” mechanism of nucleophilic vinylic substitution, a process involving 1,2-shift of the entering nucleophile (Scheme 14). This mechanism proposed at first from purely experimental evidence was then validated by quantum chemical DFT calculations. Besides, our experiments have also revealed an unexpectedly rich and varied chemistry with such compounds as **III**, **IV**, **V**, **VIII**, **IX**, **XI**, **XII** not reported previously.

It appears that, the halophilic mechanism (Scheme 2) is not the only pathway that can lead to the substitution of a heavier halogen, and the lower reactivity of **I** in the halophilic process compared to bromotrifluoroethylene [4] opens the way for the alternative “carbenoid” reaction route.

1,2-Shift of the entering nucleophile is not exactly a new idea for the NS in unsaturated systems. In fact β-addition – α-elimination – 1,2-shift sequence was among the first mechanisms to be considered for the NS in acetylenes as early as 1970s [20]. Later, it was proposed for vinylic systems to account for the substitution of a leaving group attached to the same carbon atom as the EWG-group [21], and was proved kinetically for the substitution with thiolates anions in α-bromovinylsulphones [22]. However, it remained rather a mechanistic hypothesis, and its relation to the carbenoid rearrangements has not been

explicitly considered. We have demonstrated that the realization of this mechanism depends on the nature of nucleophile involved, the ease of its 1,2-migration. This puts it among the mechanisms of nucleophilic vinylic substitution more specific for metal centered nucleophiles.

4. Experimental

General experimental techniques and procedures were exactly the same as described in the preceding communication [4]. ^1H (400 MHz), ^{19}F (376.3 MHz) and ^{13}C (100.57 MHz) NMR spectra were obtained on a Varian VXR-400 spectrometer at r.t. MALDI mass spectrum of complex **III** was obtained using a Bruker Daltonics Autoflex II spectrometer equipped with N_2 laser (337 nm), accelerating voltage 19 kV, in negative ion mode. Dithranol was used as a matrix, however similar results were obtained with anthracene. Mass spectra of other compounds were obtained under EI ionisation on a Cratos MS-890 spectrometer, operating in direct inlet method, with a source temperature of 150 °C and 70 eV ionising energy. The mass numbers of cluster peaks are given for ^{35}Cl and ^{187}Re isotopes.

Chlorotrifluoroethylene (b.p. –28 °C) was measured out by vapor pressure as described earlier [4]. The yields of the products discussed above are purely spectroscopic, based upon the relative integral intensity of the signals of the products and the signal of internal standard (PhCF_3 , $\text{C}_6\text{H}_5\text{F}$) in ^{19}F and ^1H NMR spectra of reaction solutions. The signals were referenced to the individual products by comparison to the spectra of the isolated compounds or (in case of **VII**) with the previously obtained data [4]. The parameters of NMR (^{19}F and ^1H) and IR spectra of the products are given in Tables 1 and 2, respectively (except for **V**, **VII** and **XII**). $[\text{Re}(\text{CO})_5]\text{Na}$ was purified by the low temperature crystallisation from THF, unless specially noted.

4.1. Reaction of **I** with $[\text{Re}(\text{CO})_5]\text{Na}$: the isolation of $\text{CF}_2=\text{CFRe}(\text{CO})_5$ (**II**) and $[\text{CF}_2=\text{CFRe}(\text{CO})_4\text{C}(\text{O})-\text{CFCICF}_2\text{Re}(\text{CO})_5]\text{Na}$ (**III**)

In a typical procedure a solution of 0.44 mmol of **I** in 0.26 ml THF was added to 1.33 ml of THF solution containing 0.42 mmol $[\text{Re}(\text{CO})_5]\text{Na}$ at r.t. The reaction solution was transferred into NMR sample tube, which was then frozen in liquid nitrogen and sealed off with flame. The NMR spectra showed the reaction to be completed in less than 15 min after heating to r.t. Products were isolated from a larger scale experiment, carried out with non-crystallised $[\text{Re}(\text{CO})_5]\text{Na}$, obtained from 327 mg $\text{Re}_2\text{CO}_{10}$ and 0.65 ml of 0.5% NaHg in ~8 ml THF, and 1.0 mmol **I**. After 30 min at r.t., THF was replaced with diethyl ether (2 ml), and the obtained orange solution was filtered through Celite pad. 18-Crown-6 ether (150 mg) and dioxane (0.4 ml) were consecutively added to the filtrate. The precipitation of the yellow crystals of **III**

begins immediately (a complex with 18-crown-6 and dioxane, 100 mg). The compound can be purified by dissolving in diethyl ether (3 ml) and precipitating with dioxane (0.4 ml). ^{13}C NMR (THF, r.t., δ_{C} , ppm):⁶ 252.25 dm ($\text{C}=\text{O}$, $J_{\text{d}} \sim 45$ Hz), 193.94 t ($\text{C}\equiv\text{O}$, $J_{\text{C-F}} \sim 6$ Hz, 1C), 192.45 t ($\text{C}\equiv\text{O}$, $J_{\text{C-F}} \sim 3$ Hz, 1C), 191.68 d ($\text{C}\equiv\text{O}$, $J_{\text{C-F}} \sim 8$ Hz, 1C), 191.11 m ($\text{C}\equiv\text{O}$, 1C), 183.16 t ($\text{C}\equiv\text{O}$, $J_{\text{C-F}} \sim 6$ Hz, 5C). MALDI MS (–), m/z : 822.7 $[\text{M}-\text{CO}, -\text{Na}]^-$ (5%), 800.8 (5%), 766.8 $[\text{M}-3\text{CO}, -\text{Na}]^-$ (8%), 738.8 $[\text{M}-4\text{CO}, -\text{Na}]^-$ (12%), 646.7 $[\text{Re}_2(\text{CO})_6\text{C}_4\text{F}_3]^-$ (15%), 386.8 $[\text{CF}_2=\text{CFRe}(\text{CO})_3\text{Cl}]^-$ (100%), 379.8 $[\text{CF}_2=\text{CFRe}(\text{CO})_4]^-$ (25%).

Complex **II** was isolated from mother liquor by column chromatography on silica gel (L 60/200). The first fraction eluted with petroleum ether containing $\text{Re}_2(\text{CO})_{10}$ was discarded, the second fraction eluted with petroleum ether– CH_2Cl_2 (4:1) gave 110 mg of colourless crystals. The product is extremely volatile and part of it may be lost while removing the solvent. ^{13}C NMR (THF, r.t., δ_{C} , ppm): 181.08 s br ($\text{C}\equiv\text{O}$, 4C), 182.66 d ($\text{C}\equiv\text{O}$, $J_{\text{C-F}} = 6$ Hz, 1C), 164.18 ddd ($=\text{CF}_2$, $J_{\text{C-F}} = 257, 306, 42$ Hz), 126.73 ddd ($=\text{CFRe}$, $J_{\text{C-F}} = 273, 83, 6$ Hz).

4.2. Reaction of **I** with $[\text{Re}(\text{CO})_5]\text{Na}$ in the presence of *t*-BuOH: the isolation of $\text{CHFCICF}_2\text{Re}(\text{CO})_5$ (**IV**) and $\text{F}(\text{CO})\text{CHFRe}(\text{CO})_5$ (**V**)

Alkene **I** (~1 mmol) was vacuum transferred to a NMR sample tube containing the frozen THF solution (1 ml) of 0.46 mmol $[\text{Re}(\text{CO})_5]\text{Na}$ and 58 mg *t*-BuOH. The tube was heated to r.t. and ^{19}F NMR spectra were recorded, which showed that in 8 min the reaction was completed. The products were separated by preparative TLC on Silufol-UV-254 plates eluting with CH_2Cl_2 -petroleum ether (1:1). The uppermost band contained trace amounts of $\text{Re}_2(\text{CO})_{10}$, product **IV** (25 mg) was isolated (extraction with Et_2O) from the second band ($R_f \approx 0.5$) and product **V** (51 mg) – from the bottom band ($R_f \approx 0.25$). The preparation was also repeated on a larger scale the products being separated by column chromatography on silica gel (gradient elution with petroleum ether– CH_2Cl_2). Yet in that case the isolated yield of the products was lower, especially **V** (~10%), and the colourless bands of **IV** and **V** were closely followed on the column by yellow bands of the products of their decomposition.

Crude **IV** was recrystallised from hexane (+20 to –70 °C) to give off-white solid. EI MS, m/z : 425 $[\text{M}-\text{F}]^+$ (3%), 408 $[\text{M}-\text{HCl}]^+$ (1.5%), 397 $[\text{M}-\text{F}, -\text{CO}]^+$ (9%), 381 $[\text{M}-\text{Cl}, -\text{CO}]^+$ (16%), 362 $[\text{Re}(\text{CO})_5\text{Cl}]^+$ (60%), 353 $[\text{M}-\text{Cl}, -2\text{CO}]^+$ (13%), 349 $[\text{M}-\text{CCIFH}, -\text{CO}]^+$ (34%), 346 $[\text{Re}(\text{CO})_5\text{F}]^+$ (40%), 334 $[\text{Re}(\text{CO})_4\text{Cl}]^+$ (55%), 327 $[\text{Re}(\text{CO})_5]^+$ (70%), 306 $[\text{Re}(\text{CO})_3\text{Cl}]^+$ (70%), 304 $[\text{ReCF}_2\text{CFCIH}]^+$ (80%), 299 (60%) $[\text{Re}(\text{CO})_4]^+$, 290 $[\text{Re}(\text{CO})_3\text{F}]^+$ (45%), 278 $[\text{Re}(\text{CO})_2\text{Cl}]^+$ (50%), 271

⁶ The weaker signals of fluorinated backbone were not observed.

$[\text{Re}(\text{CO})_3]^+$ (85%), 250 $[\text{ReC}_2\text{F}_2\text{H}]^+$ (45%), 243 $[\text{Re}(\text{CO})_2]^+$ (60%), 237 $[\text{ReCF}_2]^+$ (40%), 218 $[\text{ReCF}]^+$ (45%), 215 $[\text{Re}(\text{CO})]^+$ (45%), 206 $[\text{ReF}]^+$ (35%), 199 $[\text{ReC}]^+$ (50%), 187 $[\text{Re}]^+$ (100%). A peak pattern of a compound with $m/z = 714$, presumably $\text{C}_2\text{F}_4\text{Re}_2(\text{CO})_{10}$, is also observed in the spectrum except for several first scans.

Crude **V** was sublimed at $60^\circ\text{C}/5 \times 10^{-2}$ Torr to give a white solid. ^1H NMR (THF, r.t., δ , ppm): 6.184 dd ($J_{\text{H-F}}$ 51, 1.5 Hz). ^{19}F NMR (THF, r.t., δ_{F} , ppm): 9.85 d ($J_{\text{F-F}}$ 61 Hz), -184.19 dd ($J_{\text{H-F}}$ 51 Hz) -140.86 d ($J_{\text{H-F}}$ 55 Hz). EI MS, m/z : 406 M^+ (2), 359 $[\text{M-COF}]^+$ (2%), 327 $[\text{Re}(\text{CO})_5]^+$ (40%), 299 $[\text{Re}(\text{CO})_4]^+$ (50), 271 $[\text{Re}(\text{CO})_3]^+$ (90%), 243 $[\text{Re}(\text{CO})_2]^+$ (60%), 238 $[\text{ReCHF}_2]^+$ (60%), 199 $[\text{ReC}]^+$ (50%), 187 $[\text{Re}]^+$ (100%), 60 (50%), 51 (50%) $[\text{CHF}_2]^+$. Anal. Calc. for $\text{C}_7\text{HF}_2\text{O}_6\text{Re}$: C, 20.75; H 0.25. Found: C, 20.75; H, 0.26%.

4.3. Reaction of **I** with **FpK**: the isolation of **FpCCFp** (**VIII**)

FpK, obtained from 0.166 mmol **Fp**₂ and 30 μl $\text{NaK}_{2.8}$ in 4 ml THF, was mixed with **I** (0.33 mmol) in 0.15 ml THF at r.t. The solution immediately turned from orange-red to dark cherry. Part of the reaction mixture was subjected to column chromatography on silica gel, but the dark-yellow band eluted from the column with ethyl acetate– CH_2Cl_2 mixture (1:1) contained only decomposition products instead of acetylene **VIII**. The rest of the reaction mixture was placed on a column with neutral alumina (Brockman grade II), the column was first eluted with petroleum ether– CH_2Cl_2 (1:1) to remove **VII** and **Fp**₂, then a yellow band was eluted with CH_2Cl_2 –ethyl acetate (10:1) mixture which after the evaporation of the solvent afforded a few mg of a microcrystalline solid identified as **VIII**. ^1H NMR (THF, r.t., δ , ppm): 4.913. EI MS, m/z : 378 M^+ (8%), 350 $[\text{M-CO}]^+$ (10%), 322 $[\text{M-2CO}]^+$ (10%), 294 $[\text{M-3CO}]^+$ (6%), 266 $[\text{M-4CO}]^+$ (60%), 210 $[\text{M-4CO, -Fe}]^+$ (40%), 186 (80%) $[\text{FeCp}_2]^+$, 121 $[\text{FeCp}]^+$ (100%).

4.4. Reaction of **I** with **FpK** in the presence of *t*-BuOH: the isolation of **Cp(CO)FeCF=CFC(O)OBu-t** (**XI**)

Alkene **I** (0.75 g) was vacuum transferred to the frozen solution of **FpK**, obtained from 310 mg **Fp**₂ and 185 μl $\text{NaK}_{2.8}$ in 14 ml THF. The reaction mixture was allowed to thaw in cold bath (-50°C), and after stirring for 5 min heated to r.t. Metallocycle **XI** was isolated by column chromatography on silica gel. The first yellow band eluted with petroleum ether– CH_2Cl_2 mixture (8:1) contained ferrocene, it was followed by a brown band which after the removal of the solvent gave 95 mg of **XI**. m.p. 78°C . ^{13}C NMR (acetone- d_6 , r.t., δ_{C} , ppm): 228.03 dd ($J_{\text{C-F}} = 369$, 15 Hz, $=\text{CFFe}$), 218.6 d ($J_{\text{C-F}} = 2$ Hz, $\text{C}\equiv\text{O}$), 175.80 dd ($J_{\text{C-F}} = 24$, 14 Hz, $\text{C}=\text{O}$), 127.64 dd ($J_{\text{C-F}} = 277$, 9 Hz, $=\text{CF}$), 82.00 s (Cp), 28.27 s (*t*-BuO). EI MS, m/z : 312 M^+ (5%), 284 $[\text{M-CO}]^+$ (5%), 256 $[\text{M-2CO}]^+$ (2%), 228 $[\text{M-CO, -C}_4\text{H}_8]^+$ (100%), 164 $[\text{FeC}_3\text{F}_2\text{H}_2\text{O}_2]^+$ (5%), 163 $[\text{FeC}_3\text{F}_2\text{HO}_2]^+$ (4%), 140 $[\text{FeCpF}]^+$ (9%), 121

$[\text{FeCp}]^+$ (10%), 108 (29%), 89 (18%), 57 (17%), 56 (13%), 41 (17%), 39 (15%). Anal. Calc. for $\text{C}_{13}\text{H}_{14}\text{F}_2\text{FeO}_3$: C, 50.03; H 4.52. Found: C, 50.19; H, 4.60%. The saturated adduct **IX** was not isolated in this experiment, it decomposes during column or plate chromatography on silica gel.

4.4.1. Crystal data for **XI**

At 298 K crystals of **XI** ($\text{C}_{13}\text{H}_{14}\text{F}_2\text{FeO}_3$) are triclinic, space group $P\bar{1}$, $a = 8.186(3)$ Å, $b = 9.192(3)$ Å, $c = 9.560(4)$ Å, $\alpha = 76.82(3)^\circ$, $\beta = 89.43(3)^\circ$, $\gamma = 70.76(3)^\circ$, $V = 659.6(5)$ Å³, $Z = 2$ (1), $M = 312.09$, $d_{\text{calc}} = 1.571$ g cm⁻³, $\mu(\text{Mo K}\alpha) = 11.67$ cm⁻¹, $F(000) = 320$. Intensities of 3990 reflections were measured with a Siemens *P3/Pc* using graphite monochromated Mo K α radiation ($\lambda = 0.71073$ Å, $\theta/2\theta$ -scans) and 3736 independent ones were used in the further refinement. The structure was solved by direct method and refined by the full-matrix least-squares technique against F^2 in the anisotropic-isotropic approximation. Hydrogen atoms were located from the Fourier synthesis and refined using riding model. The refinement converged to $wR_2 = 0.1267$ and GOF = 0.991 for all independent reflections ($R_1 = 0.0489$ was calculated against F for 3445 observed reflections with $I > 2\sigma(I)$). All calculations were performed using SHELXTL PLUS 5.0 on IBM PC AT.

4.5. Reaction of **I** with **FpLi** in the presence of *t*-BuOH: the isolation of **CHFCICF₂Fp** (**IX**)

The solution of **FpK**, obtained from 176 mg **Fp**₂ and 120 μl $\text{NaK}_{2.8}$ in 10 ml THF, was stirred for 20 min with 51 mg LiCl, which gradually dissolved and KCl precipitated forming a light slurry. To the obtained orange-brown solution *t*-BuOH (280 mg) was added, the mixture was cooled to -50°C and 1.0 mmol of **I** (in 0.6 ml THF) was introduced. After 15 min at -50°C the reaction mixture was allowed to reach the r.t. Product **IX** (90 mg) was isolated from the reaction mixture by vacuum sublimation at $30\text{--}50^\circ\text{C}/5 \times 10^{-2}$ Torr/2 h and purified by low temperature crystallization ($+20$ to -80°C) from 2 ml petroleum ether– Et_2O (8:1). EI MS, m/z : 294 M^+ (9), 266 $[\text{M-CO}]^+$ (7%), 258 $[\text{M-HCl}]^+$ (5%), 240 $[\text{M-F, -Cl}]^+$ (5), 230 $[\text{M-HCl, -CO}]^+$ (5%), 228 $[\text{M-CFCl}]^+$ (5%), 212 $[\text{M-CO, -F, -Cl}]^+$ (8%), 205 (17%), 187 (20%) $[\text{FeCp}_2\text{H}]^+$, 186 (95%) $[\text{FeCp}_2]^+$, 177 $[\text{Fe}(\text{CO})_2\text{Cp}]^+$ (50%), 156 $[\text{FeCpCl}]^+$ (100%), 140 $[\text{FeCpF}]^+$ (95%), 121 $[\text{FeCp}]^+$ (100%), 91 $[\text{FeCl}]^+$ (55%), 82 (60%), 75 $[\text{FeF}]^+$ (85%), 65 (60%), 63 (90%), 56 $[\text{Fe}]^+$ (95%).

In the open air the solid **IX** is rapidly hydrolysed to give **Fp(CO)CHFCI** (**XII**), which was isolated as a yellow oil by column chromatography on silica gel, eluting with petroleum ether– CH_2Cl_2 –ethyl acetate (4:4:1). ^1H NMR (THF, r.t., δ , ppm): 5.085 s (Cp, 5H), 5.726 d (*CHF*, $J_{\text{H-F}} = 55$ Hz, 1H). ^{19}F NMR (THF, r.t., δ_{F} , ppm): -140.86 d ($J_{\text{H-F}} = 55$ Hz). EI MS, m/z : 205 $[\text{Fe}(\text{CO})_3\text{Cp}]^+$ (30%), 177 $[\text{Fe}(\text{CO})_2\text{Cp}]^+$ (25%), 156 $[\text{FeCpCl}]^+$ (5%), 149

$[\text{Fe}(\text{CO})\text{Cp}]^+$ (30%), 140 $[\text{FeCpF}]^+$ (5%), 121 $[\text{FeCp}]^+$ (100%), 95 (20%), 78 (80%), 56 $[\text{Fe}]^+$ (80%).

5. Computational details

Geometries were optimised using the B3LYP hybrid DFT method, using triple- ζ basis set with the Stuttgart/Dresden effective core potentials for iron and rhenium [23] and the standard 6-31G(d) basis set for other elements, as implemented in GAUSSIAN-98 program package [24]. Harmonic frequencies were calculated at the same level of theory to characterise the stationary points and transition states (at 298.15 K, 1 atm). The connectivity of the TS was confirmed by IRC calculations near the TS, followed by geometry optimization of both reactants and products. All energies are zero point corrected.

6. Supplementary material

Crystallographic data (excluding structure factors) for the structures reported in this paper have been deposited with the Cambridge Crystallographic Data Center as supplementary No. CCDC 278043. Copies of the data can be obtained free of charge on application to CCDC, 12 Union Road, Cambridge CB2 1EZ, UK (fax: (internat.) +44 1223 336 033; e-mail: deposit@ccdc.cam.ac.uk or www: <http://www.ccdc.cam.ac.uk>).

Acknowledgements

This work was financially supported by the Grant of the President of the Russian Federation for the State Support of the Leading Research Schools (Grant No. HIII-1611.2003.3). The authors gratefully acknowledge the help of Dr. Navruz G. Akhmetov in obtaining the ^{19}F and ^{13}C NMR spectra. The authors thank the P&M Company (Moscow) for a gift of chlorotrifluoroethylene.

References

- [1] Z. Rappoport, *Rec. Trav. Chim.* 104 (1985) 309.
- [2] (a) For reviews see Ref. [1] and: Z. Rappoport, *Acc. Chem. Res.* 25 (1992) 474; (b) Z. Rappoport, *Acc. Chem. Res.* 14 (1981) 7; (c) Z. Rappoport, *Adv. Phys. Org. Chem.* 7 (1969) 1.
- [3] (a) G.A. Artamkina, P.K. Sazonov, V.A. Ivushkin, I.P. Beletskaya, *Chem. Eur. J.* 4 (1998) 1169; (b) V.A. Ivushkin, P.K. Sazonov, G.A. Artamkina, I.P. Beletskaya, *J. Organomet. Chem.* 597 (2000) 77.
- [4] P.K. Sazonov, G.A. Artamkina, V.N. Khrustalev, M.Yu Antipin, I.P. Beletskaya, *J. Organomet. Chem.* 681 (2003) 59.
- [5] M.I. Bruce, P.W. Jolly, F.G.A. Stone, *J. Chem. Soc. A* (1966) 1602.
- [6] (a) K.P. Darst, C.M. Lukehart, *J. Organomet. Chem.* 171 (1979) 65; (b) D.W. Parker, M. Marsi, J.A. Gladysz, *J. Organomet. Chem.* 194 (1980) C1.
- [7] (a) C.P. Casey, D.M. Scheck, *J. Am. Chem. Soc.* 102 (1980) 2723; (b) C.P. Casey, C.J. Czerwinski, R.K. Hayashi, *Organometallics* 15 (1996) 4362.
- [8] V.F. Snegirev, K.N. Makarov, *Bull. Acad. Sci. USSR Div. Chem. Sci. (Engl. Transl.)* 35 (1986) 91.
- [9] G.A. Koutsantonis, J.P. Selegue, *J. Am. Chem. Soc.* 113 (1991) 2316.
- [10] (a) M. Akita, M. Tekada, S. Oyama, S. Sugimoto, Y. Moro-oka, *Organometallics* 10 (1991) 1561; (b) A.N. Chernega, A.J. Graham, M.L.K. Green, J. Haggitt, J. Lloyd, C.P. Mehnert, N. Metzler, J. Souter, *J. Chem. Soc., Dalton Trans.* (1997) 2293.
- [11] G. Boche, J.C.W. Lohrenz, *Chem. Rev.* 101 (2001) 697.
- [12] (a) S.P. Samuel, T.-Q. Niu, K.L. Erickson, *J. Am. Chem. Soc.* 111 (1989) 1429; (b) K.L. Erickson, *J. Org. Chem.* 38 (1973) 1463.
- [13] (a) D.L.S. Brahms, W.P. Dailey, *Chem. Rev.* 96 (1996) 1585; (b) W. Sander, G. Bucher, S. Wierlacher, *Chem. Rev.* 93 (1993) 1583.
- [14] X. Creary, M.A. Butchko, *J. Org. Chem.* 67 (2002) 112.
- [15] T.J. Barton, J. Lin, S. Ijadi-Maghsoudi, M.D. Power, X. Zhang, *J. Am. Chem. Soc.* 117 (1995) 11695.
- [16] (a) W.A. Herrmann, J. Plank, M.L. Ziegler, K. Weidenhammer, *J. Am. Chem. Soc.* 101 (1979) 3133; (b) A. Miyashita, T. Kihara, K. Nomura, N. Hiroyuki, *Chem. Lett.* (1986) 1607; (c) L.S. Hegedus, G. de Weck, S. D'Andrea, *J. Am. Chem. Soc.* 110 (1988) 2122.
- [17] (a) E.J. Crawford, C. Lambert, K.P. Menard, A.R. Cutler, *J. Am. Chem. Soc.* 107 (1985) 3130; (b) T.W. Bodnar, A.R. Cutler, *J. Am. Chem. Soc.* 105 (1983) 5926.
- [18] (a) M.N. Glukhovtsev, R.D. Bach, C.J. Nagel, *J. Phys. Chem. A* 101 (1997) 31; (b) S. Zalis, H. Stoll, E.J. Baerends, W. Kaim, *Inorg. Chem.* 38 (1999) 6101; (c) V.P. Ananikov, D.G. Musaev, K. Morokuma, *Organometallics* 20 (2001) 1652.
- [19] P.K. Sazonov, V.A. Ivushkin, G.A. Artamkina, I.P. Beletskaya, *Arkivoc* (2003) Part (X). Available from: <http://www.arkat-usa.org/ark/journal/2003/I10_Rossi-Ruveda/RR-839C/839C.pdf> and references cited therein.
- [20] H.G. Viche, S.Y. Delavarenne, *Chem. Ber.* 103 (1970) 1216.
- [21] (a) G.A. Russel, D.F. Dedolph, *J. Org. Chem.* 50 (1985) 3878; (b) B.A. Shainyan, A.N. Mirskova, V.K. Belskiy, *Zh. Org. Khim.* 22 (1986) 1923.
- [22] B.A. Shainyan, *J. Phys. Org. Chem.* 6 (1993) 59.
- [23] (a) M. Dolg, U. Wedig, H. Stoll, H. Preuss, *J. Chem. Phys.* 86 (1987) 866; (b) D. Andrae, U. Haeussermann, M. Dolg, H. Stoll, H. Preuss, *Theor. Chim. Acta* 77 (1990) 123.
- [24] M.J. Frisch, G.W. Trucks, H.B. Schlegel, G.E. Scuseria, M.A. Robb, J.R. Cheeseman, V.G. Zakrzewski, J.A. Montgomery Jr., R.E. Stratmann, J.C. Burant, S. Dapprich, J.M. Millam, A.D. Daniels, K.N. Kudin, M.C. Strain, O. Farkas, J. Tomasi, V. Barone, M. Cossi, R. Cammi, B. Mennucci, C. Pomelli, C. Adamo, S. Clifford, J. Ochterski, G.A. Petersson, P.Y. Ayala, Q. Cui, K. Morokuma, D.K. Malick, A.D. Rabuck, K. Raghavachari, J.B. Foresman, J. Cioslowski, J.V. Ortiz, A.G. Baboul, B.B. Stefanov, G. Liu, A. Liashenko, P. Piskorz, I. Komaromi, R. Gomperts, R.L. Martin, D.J. Fox, T. Keith, M.A. Al-Laham, C.Y. Peng, A. Nanayakkara, M. Challacombe, P.M.W. Gill, B. Johnson, W. Chen, M.W. Wong, J.L. Andres, C. Gonzalez, M. Head-Gordon, E.S. Replogle, J.A. Pople, *GAUSSIAN-98, Revision A.9*, Gaussian, Inc., Pittsburgh, PA, 1998.